Vaha-Savo, Lauri; Atienza, Alejandra Garrido; Cziezerski, Christian; Heino, Mikko; Haneda, Katsuyuki; Icheln, Clemens; Lu, Xiaoshu; Viljanen, Klaus

Passive Antenna Systems Embedded into a Load Bearing Wall for Improved Radio Transparency

Published in:
2020 50th European Microwave Conference, EuMC 2020

DOI:
10.23919/EuMC48046.2021.9338219

Published: 12/01/2021

Document Version
Peer reviewed version

Passive Antenna Systems Embedded into a Load Bearing Wall for Improved Radio Transparency

Lauri Vähä-Savo[1], Alejandra Garrido Atienza[1], Christian Cziezerski[1], Mikko Heino[1], Katsuyuki Haneda[1], Clemens Icheln[1], Xiaoshu Lü[2] and Klaus Viljanen[3]

[1]Aalto University School of Electrical Engineering, Finland
[2]University of Vaasa, Finland
[3]Aalto University School of Engineering, Finland
lauri.vaha-savo@aalto.fi

***Abstract* — Providing cellular network services inside residential or office buildings has become challenging, especially for fifth-generation networks that use higher carrier frequencies. Additionally, new energy-efficient buildings contain envelopes such as low-emissivity glass and new multi-layer thermal insulations, all of which – unintendedly but effectively – also block radio signals. As a solution to those problems of indoor coverage, we suggest the use of passive antenna systems embedded into the building walls. We propose a numerical evaluation method for determining the electromagnetic transmission coefficient and the thermal insulation of a typical building wall. Next, we investigate two antenna configurations embedded to the wall, a two-patch and a four-patch design, both operating around 3.5 GHz. We show from numerical simulations that those antenna systems increase the transmission coefficient of the wall. At the same time, we show that the four-patch design does not compromise the thermal insulation of the wall.**

***Keywords* — Antenna systems, energy efficient buildings, radio transparency, thermal transmittance.**

I. Introduction

Ensuring cellular radio coverage is a prerequisite in realizing ubiquitous wireless services and applications. Among different environments where cellular radios have to provide sufficient quality of services, in-building sites have become a very challenging environment nowadays, according to a subjective survey [1]. The problem becomes more serious in energy-efficient buildings equipped with highly insulated envelopes and well-sealed structures, e.g. thicker insulation layers, multi-layer heat insulation systems, low-emissivity glass, air-tight windows, and radiant barriers, all of which are also more effective in blocking radio signals [2], [3]. The energy efficiency in national and international building regulations has become significantly stricter in recent years toward the zero-energy goal as a standard practice by 2030 [4], making indoor cellular coverage by outdoor base stations even more difficult.

The challenge of indoor coverage has been addressed by several recent research activities that propose active and passive solutions. Active ones include indoor base stations, e.g., [5], and active repeaters, e.g., [6], [7], while passive ones are low-emissivity windows with frequency selective surfaces that allow microwave signal penetration [8] and signal slots [9], [10]. Active solutions may need extensive radio-frequency-over-fiber networks throughout the entire building, along with additional electricity consumption. This is particularly a problem in retrofitting a significant amount of existing buildings so that they comply with the stricter regulation of energy efficiency. Passive solutions let radio signals propagate into the building without the need of additional electricity. However, frequency-selective surfaces work only for a narrow frequency band. And while windows with slots are transparent to radio signals across wider frequency ranges, they cannot contribute much to the coverage in rooms without windows and to rooms farther away from windows. Furthermore, to the best of our knowledge, there is no commonly available design and deployment methodology for passive repeaters, especially when they are a part of a building and should operate over the building life cycle.

To tackle these challenges, we in this paper introduce a concept of passive antenna systems embedded into building walls. The antenna systems aim at letting radio signals penetrate into low-energy buildings in urban environments and hence improve cellular radio coverage provided by outdoor base stations. The main contributions of the paper are three-fold, i.e., 1) introduction of the concept of embedding antenna systems into walls, 2) simulation methodology of a typical wall that involves electromagnetic and thermal aspects and finally 3) example design of antenna systems embedded onto the wall and their electromagnetic and thermal performance. The rest of the paper is organized as follows: Section II describes definitions of walls in modern buildings. Numerical approaches to evaluate electromagnetic and thermal insulation of general wall structures are also reviewed in the section. Section III introduces an example antenna system design for a typical wall, and shows its electromagnetic and thermal performance, demonstrating its improvement in radio transparency while maintaining the original thermal insulation of the wall.

II. Electromagnetic and Thermal Insulation of a Load Bearing Wall

Building walls generally contain four principal functional layers. The layers are intended for controlling humidity, air, vapour, and heat, followed by the load bearing structure. A simple model of a typical load bearing wall structure that we use as a reference in this paper is illustrated in Fig. 1. It consists of a 220 mm-thick rock wool layer for thermal insulation (layer 2) sandwiched between 70 mm and 150 mm-thick reinforced ferroconcrete for structural bearing. Reinforcement is usually achieved with 15×15 cm metallic

Table 1. Dimensional, electrical and thermal properties of the load bearing wall

Layer # / Material	Thickness [mm]	Relative permittivity model $\epsilon_{\rm r}$ in (1) [11]	Thermal conductivity λ [W/(m · K)] [12]
#1 Concrete	70	$a = 5.31$, $b = 0$, $c = 0.0326$, $d = 0.8095$	2.3
#2 Rock wool	220	$a = 1.5$, $b = 0$, $c = 0.0005$, $d = 1.16.34$	0.035
#3 Concrete	150	$a = 5.31$, $b = 0$, $c = 0.0326$, $d = 0.08095$	2.3

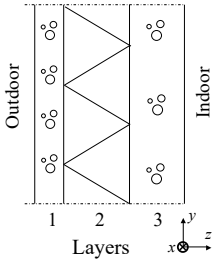

Fig. 1. A concrete sandwich panel for load bearing walls, which consists of 70 mm-thick reinforced concrete (layer 1), 220 mm-thick rock wool for thermal insulation (layer 2) and 150 mm-thick reinforced concrete for structural bearing (layer 3). Electrical and thermal parameters of each layer is summarized in Table 1.

mesh, but this differs between different buildings since the designer can implement the same load bearing capacity in many different ways.

A. Electromagnetic Insulation of the Wall

The electromagnetic insulation of the wall was numerically evaluated using CST Studio Suite [13]. In this work, the electrical properties of the materials consisting of the load bearing wall are defined according to ITU-R P.2040 [11], they are defined for popular materials in living space such as concrete and plasterboard as

$$\epsilon_{\rm r}(f\ [\mathrm{GHz}]) = \epsilon' - j\epsilon'' = af^b - j\frac{cf^d}{\epsilon_0\omega}, \tag{1}$$

where variables a, b, c and d determine frequency dependency of the permittivity, and their values are found in Table 1 according to [11]; finally, ω is angular frequency. These parameters are valid from 1 up to 100 GHz and cover the frequency range of our analyses. .

The wall is modelled as a multi-layer structure, which is infinitely large both in x and y directions. The coordinate system of the wall is defined in Fig. 1. Infinite dimensions are realized using two Floquet boundaries [14], one on the outdoor-facing side and one on the indoor-facing side. The Floquet boundary numerically extends a finite elementary cell of the wall section to virtual infinity by repeating the cell structure in $\pm x$- and $\pm y$-directions. A vertical linearly polarised incoming field is applied to the outdoor-facing Floquet port, basically representing an incoming plane wave.

Because of reflection, transmission and diffraction from the embedded antenna systems, we need to define also higher-order Floquet modes on both Floquet ports of our elementary cell, in order to capture all energy leaving the cell. Generally, higher-order modes are weaker than fundamental modes. We found that a sufficient number of modes to consider is $N_{\rm F} = 18$, at both Floquet ports of the elementary cell. The total transmission coefficient T of a plane wave applied at the outdoor-facing side is calculated by integrating those 18 meaningful modes at the port on the indoor-facing side as $T = \sqrt{\sum |T_i|^2}$, $i = 1 \cdots N_{\rm F}$.

B. Thermal Insulation of the Wall

1) Analytical Study

The thermal insulation of the wall can be represented by conductive heat flux. A steady-state density of heat flux is evaluated for a large-enough wall so that edge effects can be neglected. The heat flux depends on the structure and material of the wall as well as on temperature difference between both sides of the wall. We therefore evaluate heat transfer rate per temperature, also called a U-value and thermal transmittance. They are the inverse of thermal resistance as [15]

$$U = \frac{1}{R_{\rm tot}} = \frac{1}{R_{\rm si} + R_{\rm n} + R_{\rm se}}, \tag{2}$$

where $R_{\rm si}$ and $R_{\rm se}$ are indoor-facing and outdoor-facing thermal surface resistances. The thermal resistance is influenced by radiation of, e.g., the sun and electronic equipment, as well as air convection by, e.g., air conditioning indoors and wind outdoors. The ISO6946 standard [15] for building components and elements recommends that the evaluation is made with $R_{\rm si} = 0.13$ and $R_{\rm se} = 0.04\ \mathrm{m^2 \cdot K/W}$. Thermal resistance $R_{\rm n}$ of the wall can analytically be derived for a simple wall made of layers of N slabs by

$$R_{\rm n} = \sum_{n=1}^{N} \frac{d_{\rm n}}{\lambda_{\rm n}}, \tag{3}$$

where λ_n is a thermal conductivity $[\mathrm{m^2 \cdot K/W}]$ of layer n.[1]

2) Numerical Study

Numerical simulations of thermal transmittance were performed with Comsol Multiphysics heat transfer module [16] for the same elementary cell of the wall as in the electromagnetic simulation. As a boundary condition, we assign heat flux $q_{\rm si} = T_{\rm si}/R_{\rm si}$ and $q_{\rm se} = T_{\rm se}/R_{\rm se}$ to the indoor-facing and outdoor-facing surfaces of the wall, where $T_{\rm si} = 293$ K and $T_{\rm se} = 271$ K are the indoor-facing and outdoor-facing surface temperature, respectively. The four side surfaces of the elementary cell, i.e., other than the

[1] A symbol for thermal conductivity λ should not be confused with the wavelength of electromagnetic waves. We follow the notation of ISO6046 [15] for the symbol λ.

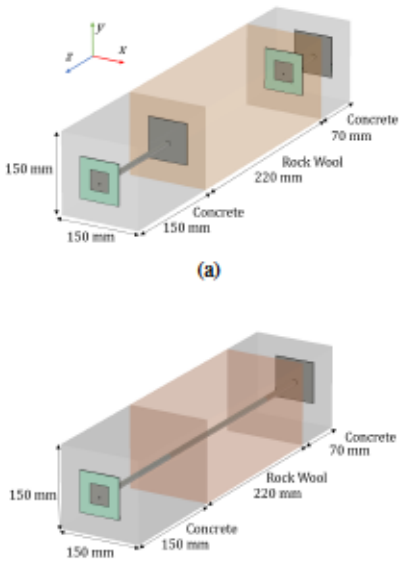

Fig. 2. Load bearing wall with embedded B2B antenna systems: (a) two B2B antenna systems across concrete layers and (b) a B2B antenna system going through the entire wall.

indoor-facing and outdoor-facing surfaces, are defined to be thermal insulation boundaries so that the wall is virtually infinitely large along x and y directions according to the coordinate system in Fig. 1. The thermal insulation boundaries ensure no conductive heat flux normal to the four side surfaces and hence the temperature on the indoor-facing and outdoor-facing wall surfaces is constant. Thermal conductivity values for each layer of the load bearing wall in Fig. 1 are found in Table 1.

III. Embedding Back-to-Back Antenna Systems into Walls

This section elaborates a design of back-to-back antenna systems embedded into the reference wall, contributing to improved radio transparency of the wall. Their influence on thermal insulation is also analyzed.

A. Design of Antenna Systems

As an exemplary antenna system embedded into a load bearing wall, we consider back-to-back patch antennas resonating at a possible fifth-generation cellular band of 3.5 GHz. There are two different designs of squared patches, one facing outdoor and indoor space and hence matched to the air, and another embedded into the inner part of the wall and matched to rock wool. Patch antennas are designed on Rogers RO3003 substrate with $\epsilon_r = 3.0$. Antennas are connected to each other via a coaxial cable, where the feeding position is $(x, y) = (0, -3)$ mm for the center-located elementary cell. The coaxial cable and patch antenna dimensions are summarized in Table 2.

We considered two types of back-to-back antenna systems, illustrated in Fig. 2. The one in Fig. 2a adopts two back-to-back patch antenna systems, each going through one of concrete layers; the rock-wool layer remains intact. The one in Fig. 2b has a coaxial cable going through the entire wall; these are referred to as *four-* and *two-patch designs* hereinafter. We show electromagnetic and thermal properties of antenna-embedded load bearing walls with two- and four-patch designs in the following subsections.

Table 2. Optimized dimensions of 3.5 GHz microstrip patch antennas

Parameter	Symbol	Dim.(mm)
Patch width, facing air	w_a	23.7
Patch width, facing rock wool	w_r	23.2
Substrate width	w_s	50
Substrate thickness	t_s	1
Metal thickness	t_m	0.035
Coaxial cable inner radius	r_{in}	1
Coaxial cable outer radius	r_{out}	3.35
Coaxial cable dielectric radius	r_{diel}	2

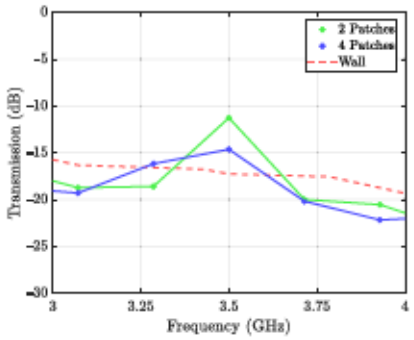

Fig. 3. Electromagnetic insulation of the load bearing wall in Fig. 1, along with those embedding back-to-back antenna systems. In this example, antenna systems are embedded at every 150 mm on the wall.

B. Electromagnetic Insulation of Antenna-Embedded Wall

Figure 3 illustrates electromagnetic insulation of antenna-embedded load bearing wall with two- and four-patch designs. Dimension of the antenna-embedded elementary cell is $150 \times 150\text{mm}^2$. Both cases show narrow bandwidth of designed patch antennas resonating around 3.5 GHz. Out of this band, electromagnetic insulation becomes higher than for the original wall because the ground plane reflects part of the incident field. For the antenna-embedded wall, the attenuation of transmitted fields is reduced by 6 dB and 2.7 dB at 3.5 GHz for the two- and four-patch designs, leading to the transmission coefficients of -11.3 and -14.6 dB, respectively.

C. Thermal Insulation of Antenna-Embedded Wall

The thermal insulation was simulated for these antenna structures using the same elementary cell sizes as the electromagnetic simulations. The reference wall has a U-value of 0.15 $\text{W}/(\text{m}^2\text{K})$. The wall with the two-patch design degrades a U-value to 0.51 $\text{W}/(\text{m}^2\text{K})$, which is higher than allowed for building walls in Finland [17] and therefore is not a good solution in terms of thermal insulation. On the other hand, the four-patch design maintains a U-value of 0.15 $\text{W}/(\text{m}^2\text{K})$.

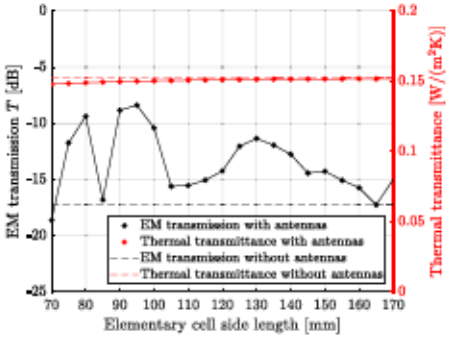

Fig. 4. Electromagnetic and thermal insulation of antenna-embedded wall shown in Fig. 2a for varying elementary cell size for the four-patch antenna-embedded wall shown in Fig. 2a as a function of elementary cell size.

D. Impacts of Antenna Tile Areas on Electromagnetic and Thermal Insulation

Figure 4 shows the variation of the electromagnetic (left y-axis) and the thermal (right y-axis) insulation when the elementary cell size varies from 70 mm to 170 mm with the four-patch design. We can observe fluctuations in the electromagnetic transmission, mainly due to the standing waves that occur in the rock-wool layer and due to a single antenna coupled with multiple other antennas in the same layer. As expected, these interferences are reduced when the elementary cell size is increased.

The U-value decreases slightly when the elementary cell size is increased. This unexpected decrease can be explained by the fact that Rogers RO3003 PCB material used in the patch antennas has a low thermal conductivity of 0.5 $\mathrm{W/(m \cdot K)}$ and hence acts as an additional thermal insulator on top of the concrete. When elementary cell sizes is change from 70 mm to 170 mm the antenna tiles cover 51 to 8.5 % of the wall. Hence, with large elementary cell size, the U-value approaches one of the reference wall. However, the U-value changes only very slightly with elementary cell size and with this design we always get at least the same U-value as the reference wall.

IV. Concluding Remarks

This paper introduces a simulation method for antenna systems embedded into a load bearing wall. Two different antenna solutions were simulated, showing that the electromagnetic attenuation is decreased by up to 6 dB with shown antenna configuration. Also, the thermal insulation evaluated through U-value showed that adding antennas and coaxial cables only to the concrete layers of the wall maintains the thermal insulation, while the U-value becomes unacceptably high if a cable goes through the entire wall.

As a future perspective, we will study the influence of embedding different antenna systems also on other essential figures-of-merit of walls, e.g., structural solidity and acoustic insulation.

Acknowledgement

The work has been supported by the Academy of Finland Research Project "Signal-Transmissive-Walls with Embedded Passive Antennas for Radio-Connected Low-Energy Urban Buildings (STARCLUB)," decision #323896.

References

[1] Zinwave, "Cellular in the workplace survey, 2017 connectivity issues are widespread," 2017. [Online]. Available: https://www.cei-das.com/wp-content/uploads/Zinwave-Survey-Report-LP.pdf

[2] I. Rodriguez, H. C. Nguyen, N. T. K. Jorgensen, T. B. Sorensen, and P. Mogensen, "Radio propagation into modern buildings: Attenuation measurements in the range from 800 MHz to 18 GHz," in *Proc. 2014 IEEE 80th Veh. Tech. Conf. (VTC2014-Fall)*, Sep. 2014, pp. 1–5.

[3] K. Haneda et al., "5G 3GPP-like channel models for outdoor urban microcellular and macrocellular environments," in *Proc. IEEE 83rd Vehicular Technology Conference (VTC Spring)*, May 2016, pp. 1–7.

[4] European Commission, "European union directive on nearly zero-energy buildings," 2019. [Online]. Available: http://ec.europa.eu/energy/en/topics/energy-efficiency/buildings /nearly-zero-energy-buildings

[5] S. F. Yunas, "Capacity, energy-efficiency and cost-efficiency aspects of future mobile network deployment solutions," doctoral dissertation, Tampere University of Technology, Oct. 2015.

[6] K. Haneda, E. Kahra, S. Wyne, C. Icheln, and P. Vainikainen, "Measurement of loop-back interference channels for outdoor-to-indoor full-duplex radio relays," in *Proc. 4th European Conf. Ant. Prop.*, Barcelona, Spain, Apr. 2010, pp. 1–5.

[7] J. M. Rigelsford, K. L. Ford, and L. Subrt, "A passive system for increasing cellular coverage within energy efficient buildings," in *Proc. The 8th European Conf. Ant. Prop. (EuCAP 2014)*, Apr. 2014, pp. 614–615.

[8] A. Asp, A. Baniya, S. F. Yunas, J. Niemelae, and M. Valkama, "Applicability of frequency selective surfaces to enhance mobile network coverage in future energy-efficient built environments," in *Proc. 21th European Wireless 2015*, May 2015, pp. 1–8.

[9] Lammin Windows & Doors, "Signal window." [Online]. Available: http://signal-window.com/

[10] J. Lilja, "Mobile-friendly glass –comparing solutions from the end user viewpoint," in *Proc. Glass Performance Days 2019 (GPD2019)*, Tampere, Finland, June 2019.

[11] Recommendation ITU-R P.2040, "Effects of building materials and structures on radiowave propagation above about 100 MHz," July 2015. [Online]. Available: https://www.itu.int/dms_pubrec/itu-r/rec/p/ R-REC-P.2040-1-201507-PDF-E.pdf

[12] European Standard, "ISO 10456:2007 - Building materials and products - Hygrothermal properties - Tabulated design values and procedures for determining declared and design thermal values," Feb. 2017.

[13] CST Studio Suite©, www.cst.com. Dassault Systèmes, Vélizy-Villacoublay, France.

[14] E. Richalot, M. Bonilla, M.-F. Wong, V. Fouad-Hanna, H. Baudrand, and J. Wiart, "Electromagnetic propagation into reinforced-concrete walls," *IEEE Trans. Microwave Theory. Tech.*, vol. 48, no. 3, pp. 357–366, 2000.

[15] European Standard, "ISO 6946:2017 - Building components and building elements - Thermal resistance and thermal transmittance - Calculation methods," Feb. 2017.

[16] COMSOL Multiphysics© v. 5.5., www.comsol.com. COMSOL AB, Stockholm, Sweden.

[17] Ministry of the Environment of Finlad, "1010/2017 Decree of the Ministry of the Environment on the Energy Performance of New Buildings," Dec. 2017. [Online]. Available: https://www.ym.fi/en-US/Land_use_and_building/Legislation_and_ instructions/The_National_Building_Code_of_Finland/ Energy_efficiency_of_buildings